Othmane MAAKOUL[1*], Ruth BEAULANDA[1], Hamid El OMARI[1], Aziza ABID[2], Elhassane ESSABRI[1].

J. Electrical Systems 16-4 (2020): 582-603

Modeling and optimal energy management of a micro-hybrid-grid, equipped with a renewable energy source, a conventional source, and a cogeneration unit.

Journal of Electrical Systems

Abstract: Our objective through this work is to have a cogeneration system integrated into a hybrid production system, coupled to the public grid and equipped with an ecological production system (photovoltaic) with a storage system (accumulator), and to establish rules and tools for optimizing energy management as well as the dimensioning of an energy system. The optimizations will be carried out on the basis of consumption and production data. The optimization criterion will be economic with a view to minimizing the total cost of the system to meet the energy demand of a typical profile during a basic test period. However, "optimal" sizing requires coordination with effective energy management to identify the optimum power references, the minimum and maximum powers provided by each source and to estimate the depth of discharge of the storage element. The parts presented concern the dimensioning and management of energy transfers on the basis of consumption data and tariffs are:
- Establishing reliable and adapted electrical models of the subsystems. In order to be able to determine, at each moment, for a given consumption and a given deposit, the power that the production systems can provide. These models must be sufficiently accurate to account for energy transfers and fast enough to allow calculations over long periods of time.
- Establish economic models of the different modules of the system. Climate deposits, consumption profiles, fuel consumption, energy efficiency of the systems.
- Finally, carry out economic and energy optimization studies of the energy system using micro-grid management algorithms based on different configurations of the system

Keywords: modelling; micro-grid; renewable energy; energy system; cogeneration system; photovoltaic; public grid; optimizing energy management; dimensioning; storage system

Article history: Received 14 April 2020, Accepted 1 October 2020

1. Introduction

The problems of energy supply and environmental protection are today of great importance in the world. On the one hand, reserves of fossil resources (oil, natural gas, coal) are limited and on the other hand, the use of these resources is responsible for the increase in greenhouse gas (GHG) concentrations in the atmosphere, leading to global warming [1][2]. In the framework of the debates on energy transition, the hybridization of production sources and their implementation in the public grid is put forward as part of the solution to address both climate and energy issues.

A hybrid system is an electrical grid that autonomously coordinates the production, consumption and storage of electrical energy [3]. This type of network therefore makes it possible to move from a demand-driven production system to a consumption system based on other constraints such as electricity supply and feed-in tariffs, which in the future will have to adapt to random variations in the production of renewable energies (solar, wind, biomass...), this network must contribute to improving security of supply, to reduce the costs of the distribution network and control energy, to integrate renewable energies into the grid and to improve the efficiency of the whole system, if several technologies can be used, they

* Corresponding author: Othmane MAAKOUL, E-mail: othmane.1992.mkl@gmail.com
1: Laboratory of Renewable Energies Environment and Development, Hassan 1st University, Faculty of Science and Technology Settat City, Morocco
2: National School of applied sciences, Moulay Slimane University, Khouribga City, Morocco

Copyright © JES 2020 on-line : journal.esrgroups.org/jes

should first be tested as individual components to study the stability and efficiency of their interaction [4].

In this context cogeneration systems have emerged as a solution to help approve demand during peak hours, as well as to compensate for other renewable energies that are intermittent and dependent on climatic conditions such as solar and wind. Cogeneration technology, also known as combined energy production, is a technique for the simultaneous production of electricity and heat, its interest lies in the higher energy yields obtained compared to equivalent separate production of electricity and heat [5], thus it allows to reduce emissions of polluting gases when it is fed by fuels of a renewable nature such as purified biogas. This technique is used in isolated or grid-connected sites. It consists of an internal combustion engine, which burns fuel to create a mechanical movement, it is coupled to a synchronous generator that transforms this mechanical movement into electrical energy, plus heat exchangers to recover thermal energy in the cooling and exhaust systems.

The implementation of such a system aims to diversify the sources of renewable energy, thus seeking a more significant reduction in the electricity bill consumed since renewable sources can complement each other and provide a greater amount of energy. Part of the work is oriented towards the physical modelling of electrical production systems (photovoltaic chain, cogeneration unit...), there is also an optimization study of the system configuration according to various criteria: combination of a minimal cost of the system for a requested power [6]. The complexity of hybrid systems makes decision making difficult. However, an intelligent control strategy is needed to manage the behaviour and power distribution of the multi-source system. These energy sources must supply the load according to its needs while respecting the various constraints related to the operation of the sources (production, maximum power, efficiency, energy losses) and the storage elements (state of charge, dynamics, ageing).

2. System model

Before a control strategy for energy management can be implemented, in order to plan the energy flows of the micro-grid in an optimal way, the different production components making up the system must be modeled. This representation must be adapted, in terms of granularity, in relation to the management algorithms developed and the associated simulation times. The following components are typically included in our designed system: centralized power grid, large capacity battery (energy storage), local cogeneration as a back-up means of production (simultaneous production of heat and energy), and a production source of a renewable nature (solar photovoltaic).

The system model is shown in Figure 1. In order to be compatible in terms of complexity with the optimization procedures that will be developed, the network is modeled at a fairly high level in terms of energy flows without consideration of voltage/current and control loops.

The ratings used and the parameters characterizing each of these entities are described below:

- The consumer (individual, local authority, industry...) needs a certain amount of energy for his own consumption at any given moment. Its consumption, in power, is noted $P_c(t)$

- The producer of renewable energy produces at time *t* a power $P_1(t)$. This power depends:
  - The solar deposit whose temporal distribution is given by the function $G_{PV}(t)$ (sunshine in W/m²).
  - The ambient temperature *Ta(t)* in °C
  - The production capacity in terms of installed peak power.
  - Transfer functions (relations between the weather and electrical conditions and the electrical production) a solar conversion chain noted F_{PV};
  - The reversible inverter is characterized by the power transiting through it at time t, and 1, its conversion efficiency;
- A local cogeneration unit for the production of electricity powered by a renewable energy source (biogas).
- Availability of generation systems rated *A(t)* in case of maintenance or failure;

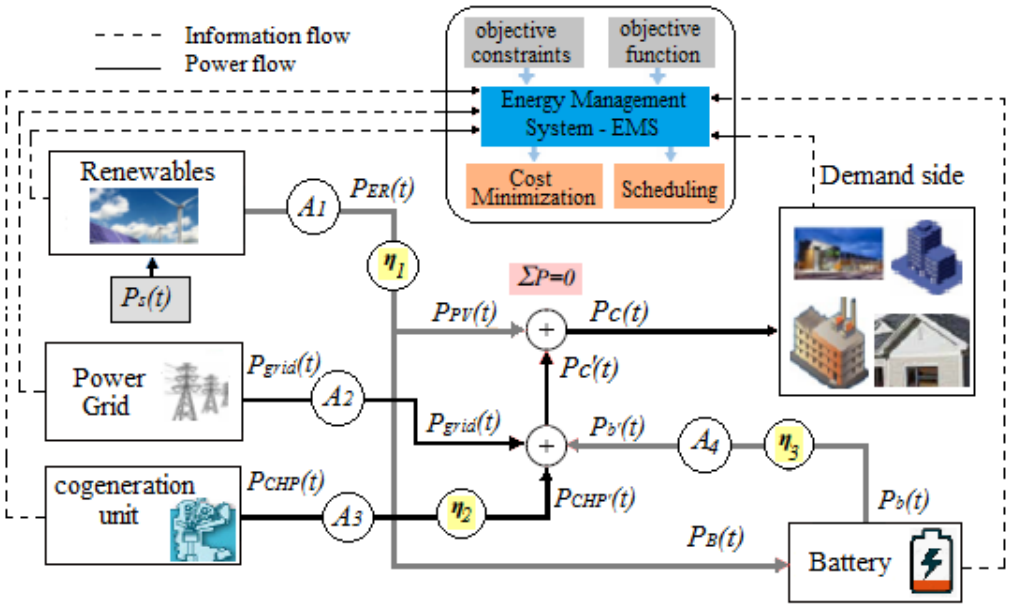

Figure 1: Overview diagram of the production system

3. Modeling of system elements

Studies of the different structures of renewable energy hybrid systems are carried out on the basis of various models depending on the objective [7][8]. These models have in common the use of meteorological data as input variables for the case of the photovoltaic system. These data have to reflect the actual energy input received, which requires that the most often available data be converted into usable data (solar irradiation, temperature...) [9][10]. In the following, the models of both the photovoltaic and cogeneration converters and the electronic converter are briefly described. The modeling of energy production systems aims first of all at obtaining a tool for dimensioning and investigating the real physical system [11]. Several works have been carried out on the subject [12], depending on the goal; the studied systems will be described by more or less complex dynamic equations. In this section, we will present some information related to the subsystems constituting a hybrid system and their numerical simulation under the Matlab/Simulink environment.

3.1. Models of the photovoltaic system

The behavior of photovoltaic modules has been studied at length in the work of [13][14]. In the literature, there are two types of PV module models: electrical and energy models. The electrical model is called diode-equivalent model (the most commonly used) or two-diode equivalent model [15][16][17]. In this approach the supplied current and the terminal voltage of the module are calculated from the received solar irradiance, the ambient temperature It can be applied in short-term process studies, when it is necessary to know the electrical quantities or to calculate the output power of the photovoltaic system

The current delivered by a photovoltaic cell:

$$I_G = P_1.E_s[1 + P_2(E_s - E_{ref}) + P_3(T_j - T_{jref})] - P_4.T_j^3.\exp(-\frac{E_g}{k.T_j}).[\exp(\frac{q}{k.A.n_s.T_j}(V_G + R_S.I_G)) - 1] - \frac{V_G}{R_{sh}} \quad (1)$$

In the study we will conduct, the photovoltaic field will be connected to a MPPT (*Maximum Power Point Tracker*) [18][19], which allows to recover the maximum available solar power.

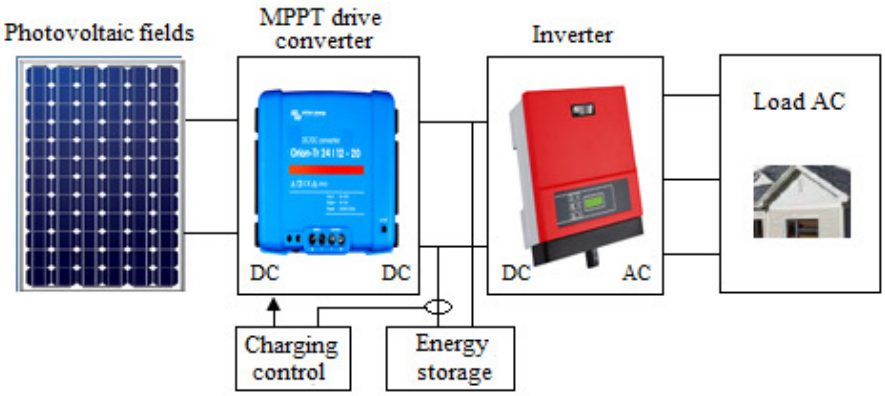

Figure 2: Photovoltaic production chain

The integration of the MPPT simplifies the simple diode model to a single empirical equation. Now, using only the climatic data of the site (sunshine and ambient temperature) and the data of the module manufacturer, we can know the maximum power available at the output of the *PV* module [19][20]. It is assumed that all the modules composing the *PV* field are subject to the same weather conditions and behave in a similar way with regard to the PV field surfaces. This model does not take into account the connection losses between the modules. The energy produced by a *PV* field is estimated from the overall insolation on the inclined plane $I_g(t)$ in W/m^2 , the ambient temperature, and the characteristics of the module provided by the manufacturer under standard conditions.

$$P_{MPPT} = N_{PV}.\frac{G_I}{G_I^R}[P_{max} + \mu_{max}.(T_J - T_J^R)] \quad (2)$$

$$T_J = T_A + G_I.\frac{NOCT-20}{800} \quad (3)$$

Knowing that the efficiency (under standard conditions) of a module is given by the relationship:

$$\eta_{PV} = \frac{P_{PV-crete}}{G_I^R .S_{PV}} \tag{4}$$

Calculating the size of the battery bank:

To make up for the lack or excess power, the system has a Lithium-Ion battery bank, with a nominal voltage of V_{batt} imposed by the test bench. The capacity of the storage battery bank in a hybrid system depends on the maximum daily charge, the number of days of autonomy, and the maximum discharge [17][19]. It is calculated by the expression:

$$C_{batt} = \frac{J.E_c(t)}{\eta_{batt}.V_{batt}.DOD} \tag{5}$$

The inverter is an electronic converter whose purpose is the transformation of an electric power in direct current, produced by the photovoltaic installation, into a power in alternating current which will be supplied to the electric network or feed the isolated load. The efficiency of the converter η_{inv} depends on the load, i.e. on the AC output power P_{out}. [21][22] This dependency is called the inverter load curve and will be used for the analysis of the operation of hybrid systems under steady state conditions. For the DC/AC inverter, the DC input power (which is the power produced by the PV modules) is known and not the output power. Therefore it is necessary to express the efficiency as a function of the input power. The reduced electrical losses ploss can be expressed with satisfactory accuracy by a constant, load-independent component p_0 (%) and a load-dependent component p_0 (%) [21][22]. The expression is presented in equation (6):

$$p_{loss} = \frac{P_{loss}}{P_{inv,rated}} = p_0 + k.p^2 \tag{6}$$

Where Ploss are the electrical losses, $P_{inv,rated}$ is the nominal power of the inverter, p_0 and k are coefficients calculated from the data provided by the manufacturer by equations (7) and (8):

$$p_0 = \frac{1}{99}\left(\frac{1}{\eta_{10}} - \frac{1}{\eta_{100}} - 9\right) \tag{7}$$

$$k = \left(\frac{1}{\eta_{100}}\right) - p_0 - 1 \tag{8}$$

Where η_{10} and η_{100} are the efficiencies respectively at 10 and 100% load with respect to the nominal power, provided by the manufacturer. The reduced power p is expressed by (9).

$$p = \frac{P_{out}}{P_{inv,rated}} \tag{9}$$

The electrical losses are the difference between the Pin input DC power and the output power (10). Thus combining equation (6) and (10) we get (11):

$$P_{loss} = P_{in} - P_{out} \tag{10}$$

$$(p_0 + k.p^2)P_{inv,rated} = P_{in} - P_{out} \tag{11}$$

On the other hand, the input power can be expressed from the output power and efficiency (12). Thus after substituting (12) in (11) and using (9) one obtains (13):

$$P_{inv} = \frac{P_{out}}{\eta_{inv}} \tag{12}$$

$$p_0 + k.p^2 = \frac{p}{\eta_{inv}} - p \tag{13}$$

Hence the efficiency of the inverter is expressed by (14):

$$\eta_{inv} = \frac{p}{p_0 + k.p^2 + p} \tag{14}$$

3.2. Modeling a cogeneration unit

A diesel generator can be divided into three main components: the main engine, which consists of a machine (internal combustion engine) with a speed governor that rotates the inductor of a synchronous generator (alternator), and an automatic voltage regulator (control system) that keeps the whole unit stable [23]. This system is the seat of a set of very different phenomena (electrical, electromechanical, mechanical, thermochemical, etc.), difficult to describe by simple dynamic equations. In the literature the modeling of a cogeneration unit generally focuses on mechanical, electromechanical and electrical phenomena. However, these models are often parameterized by thermochemical considerations related to the thermodynamic cycle of the heat engine [24].

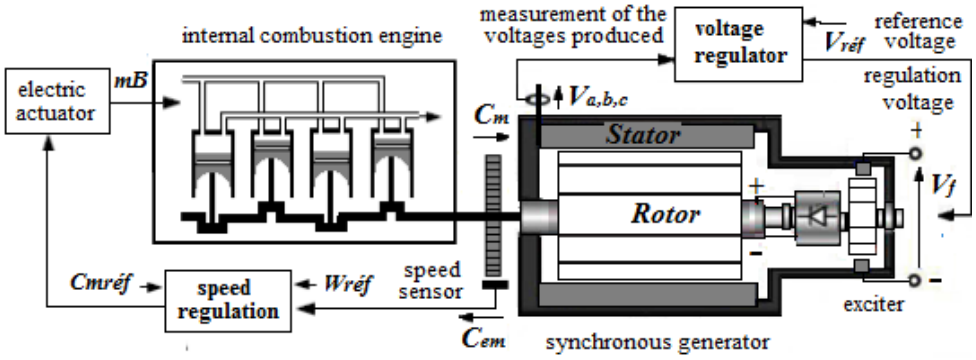

Figure 3: Model of a cogeneration system

Renewable energy systems have intermittent output characteristics and are integrated with conventional energy sources to provide constant power. In many hybrid systems, the diesel generator acts as this stable source of power. Diesel generators are designed to satisfy the load and also to charge the storage device (battery) when the power supplied by the renewable energy source and the battery is insufficient to satisfy the load. An adequate energy balance is necessary for the optimal operation of such a system [25][26].

3.2.1. Mechanical torque generation

In this section focusing on the dynamics of mechanical torque in relation to the fuel flow index [27][28].

$$C(s) = \frac{K}{1 + s.T_r}.m_B(s).e^{-s.T_c} \tag{15}$$

$$\frac{d\omega_m}{dt} = \frac{1}{2H_D}(C_m - C_{em} - D_D.\omega_m) \tag{16}$$

$$H_D = \frac{1}{2}.\frac{J_D.\omega^2 mref}{S_{ref}} \tag{17}$$

The instantaneous electrical power produced by the generator is written [29]:

$$P_g = (V_S^{dqo})^T.I_s^{abc} = \frac{3}{2}(V_d.i_d + V_q.i_q + 2V_o.i_o) \tag{18}$$

$$P_g = \frac{3}{2}\left[\left(i_d.\frac{d\varphi_d}{dt} + i_q.\frac{d\varphi_q}{dt} + 2i_o.\frac{d\varphi_o}{dt}\right) + (\varphi_d.i_q - \varphi_q.i_d)\omega_e - (i_d^2 + i_d^2 + 2i_o^2)R_a\right] \tag{19}$$

[Variation in armature magnetic energy] [Electromagnetic power] [Joules loss]

Electromagnetic power is the power transmitted through the air gap. By dividing this power by the driving speed of the rotor (m=sync), we obtain the electromagnetic torque of the generator (this torque will be opposed to the mechanical torque of the combustion engine of the cogeneration unit).

$$C_{em} = \frac{3}{2}.(\varphi_d.i_q - \varphi_q.i_d)\frac{\omega_e}{\omega_m} \tag{20}$$

3.2.2. Hourly fuel consumption

For a cogeneration group, the hourly fuel consumption is strongly related to the load rate and the rated power of the generator, can be approximated by a linear function of the load rate [23][24][30][31]:

$$m(t) = (a_0 + a_1\delta)P_3(t) \tag{21}$$

With ***m***: Hourly fuel consumption, usually expressed in (L/h)

a₀, a₁: Constants obtained from literature or experiments (L/KWh)

It is interesting to study the optimal management of CHP generators by seeking to minimize fuel consumption. The number of generators required can be expressed as a function of maximum power. Since a hybrid system must be able to provide part of the load even in the absence of sunshine (cloudy or night-time passages), with a lack of electrical grid, the total number of generators can be determined by the expression [23]:

$$N_{CHP} = \frac{\max(P_{max}(t))}{P_{e-CHP}(t)} \tag{22}$$

Since the generators are all identical, the fuel consumption and the total power of the load to be supplied by the local cogeneration units at time t are written respectively:

$$m(t) = P_{e-CHP}(t).\sum_{N_{on}(t)}^{N_D}(a_0 + a_1\delta_j(t)) \tag{23}$$

$$P_{T-CHP}(t) = P_{e-CHP}(t).\sum_{N_{on}(t)}^{N_D}\delta_j(t) \tag{24}$$

Where $N_o(t)$ is the number of generators in operation at time *t*, and N_D is the total number of cogeneration units installed, noting that $N_o(t) < N_D$

According to expressions (23) and (24), fuel consumption is written as follows:

$$m(t) = P_{e-CHP}(t)\left[N_{on}(t).a_0 + a_1 \sum_{N_{on}(t)}^{N_D} \delta_j(t)\right]$$

$$= N_{on}(t).a_0.P_{e-CHP}(t) + a_1.P_{T-CHP}(t) \quad (25)$$

Equation (25) shows that minimizing the number of generators in operation each hour will also result in minimizing fuel consumption [23]. Therefore, the number of generators in operation $N_O(t)$ can be determined by :

$$N_{on}(t) = \frac{P_{CHP}(t)}{P_{e-CHP}(t)} \quad (26)$$

With an hourly time step (Δt= 1h), the average daily running time T of each generator will simply be written:

$$T = \sum_{24} N_{on}(t).\Delta t\ /N_D \quad (27)$$

In the case where all generators are identical and all coupled in parallel, the equilibrium point will naturally go to a state where all load rates have the same value. Thus, at each instant t, the charge rate can be determined by [23]:

$$\delta(t) = \frac{P_{T-CHP}(t)}{N_{on}(t).P_{e-CHP}(t)} \quad (28)$$

3.3. Numerical simulation of the two PV/CHP production sources

For the simulation, the first source consists of a photovoltaic system connected in series with a partial MPPT to recover the maximum of the power produced, keeping a constant voltage at its output, the second source is equipped with a cogeneration group connected in series with a controlled rectifier. The two sources are connected in parallel with each other. At the output of the two sources there is a global chopper to control the power to be injected into the electrical grid. The simulation diagram under the Matlab/Simulink software, presents the two production sources, plus the conversion chain which consists of a global chopper, and an inverter for the conversion of the voltage generated by the global chopper into sinusoidal voltages at the output, and the synchronization of the latter with the voltages coming from the electrical grid.

The model is applied to Matlab-Simulink. A series of simulations is carried out to study the behavior of the model, simulation parameters Settings: rated output power of synchronous generators is 4KW; Rated voltage is 380V; Frequency is 50Hz;

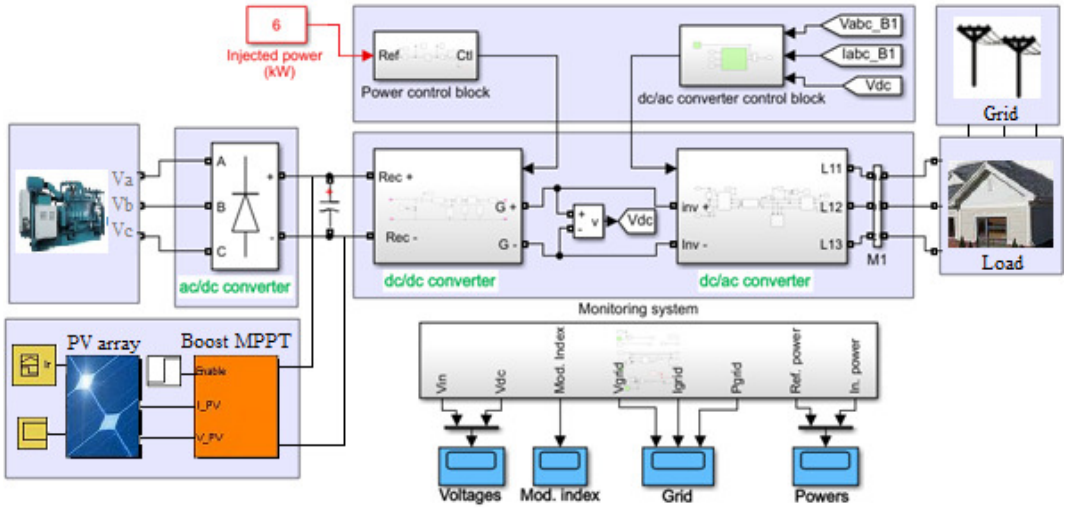

Figure 4: synoptic schematic of system modeling under the Matlab/Simulink environment

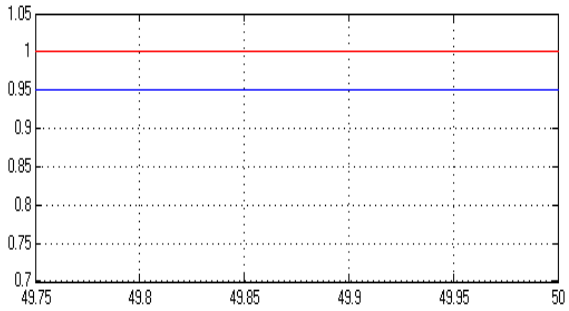

Figure 5: Reference and measured mechanical torque $C_{m\text{-}ref}$ (red) and $C_{m\text{-}mesured}$ (bleu) in reduced value

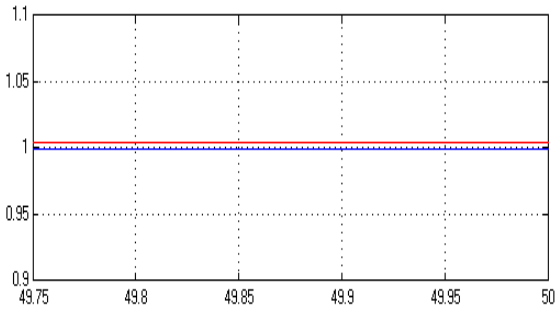

Figure 6: Mechanical reference speed and measured $\omega_{n\text{-}ref}$ (bleu) and $\omega_{n\text{-}mesured}$ (red)

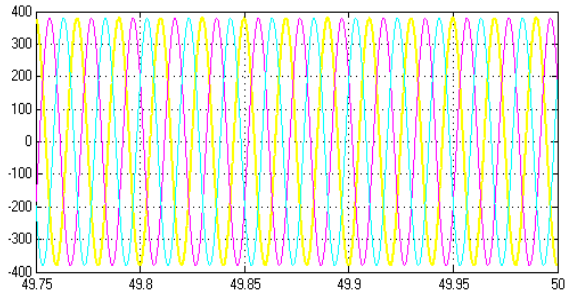

Figure 7: The stator voltages of the synchronous generator $V_{a,b,c}$

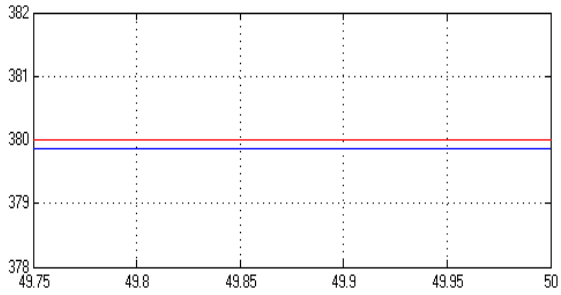

Figure 8: Voltage set-point (red) and measured voltage (bleu) of the voltage regulator

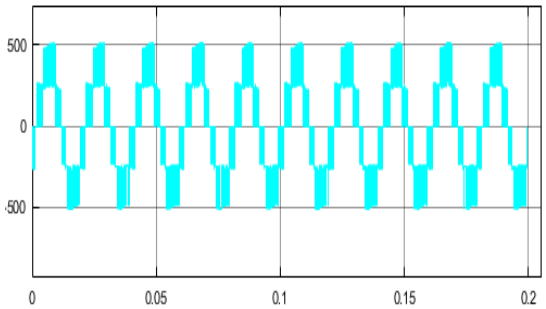

Figure 9: Voltage at the output of the inverter before filtering

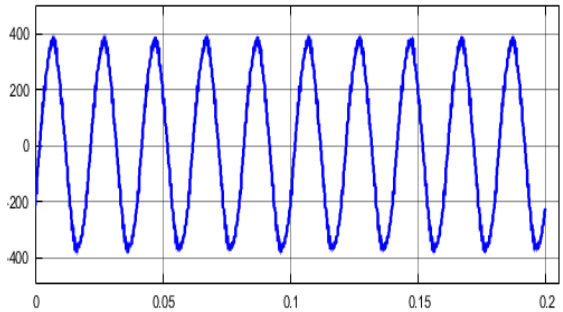

Figure 10: Voltage at the output of the inverter after filtering

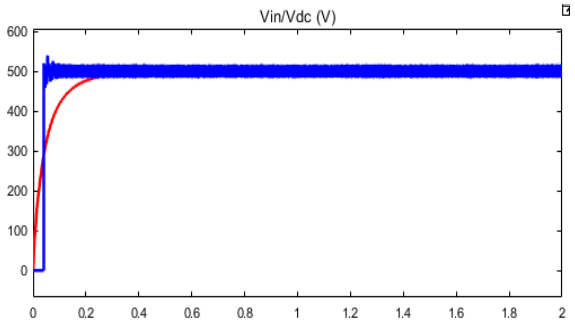

Figure 11: DC bus voltage regulated to 500V

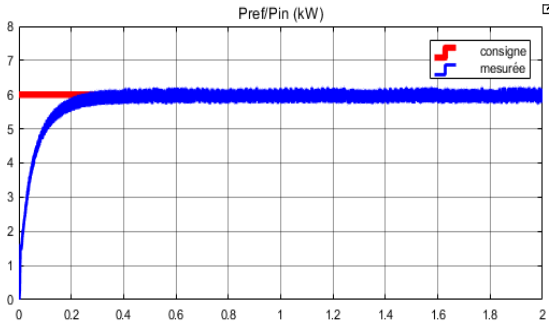

Figure 12: The power at the output of the system regulated on 6KW

The response of the system at constant (reduced) speed and torque is given in Figures 5 and 6; both graphs show that the speed governor of the internal combustion engine is correctly defined.

Figure 8: The regulation voltage is maintained around 379 and 380 V. This explains why the functions of the different controls have been correctly realized either for the excitation system or for the voltage regulator.

Figure 7: the behavior of the system is a balanced three-phase system, which means that the proposed simulated model is quite efficient. Figure 11 shows the voltage at the output of the boost in relation to a reference value of 500V, the figure shows that the measured voltage is very close to the set value.

Figure 12: gives the value of the electrical power generated by the cogeneration system, indicating that the current and voltage control loops in the conversion chain have been well defined.

4. Economic modeling

The optimization of energy transfers and installed power will be done according to economic criteria. We must therefore introduce a cost function for the user of each element of the complete system [20]. In a general way, we define the operating cost $C_{total}(t)$ by a given element at time "t" (t in hours), as the sum of the C_I investment costs (depends on the maximum capacity of the elements), C_E energy (This cost depends on the power produced or consumed at time t and the maximum power that can be received or returned by the element, and C_U use (This cost can be broken down into an annual maintenance cost that depends on the capacity of the installation and a production-dependent wear and tear maintenance cost) [32][33]. The total cost of operating the system is:

$$C_{total} = \sum C_I(t) + \sum C_E(t) + \sum C_U(t) \tag{29}$$

The operating cost of the components can also be included in the system management strategy: fuel cost for connected *CHP* units. Often these costs are estimated in a linear way according to the power delivered by the sources concerned.

- *For the production system: renewable energy*

$$C_{PV} = \sum_{t=1}^{24} \frac{C_{I-PV}(P_{PV-crête},t)}{T_{PV-vie}}.t + \sum_{t=1}^{24} C_{m-PV}.A_1(t).P_{PV}(t) \tag{30}$$

C_{I-PV} : The total investment cost in (€/KW) for a lifetime T_{PV-vie} in (hour)
C_{m-PV} : Maintenance cost (€/h)

- *For the cogeneration unit:*

$$C_{CHP} = \sum_{t=1}^{24} \frac{C_{I-CHP}(P_{CHP-crête},t)}{T_{CHP-vie}}.t + \sum_{t=1}^{24} C_{m-CHP}.A_3(t).P_{CHP}(t) + \sum_{t=1}^{24} C_{u-CHP}.A_3(t).P_{CHP}(t) \quad (31)$$

C_{I-CHP} : The total investment cost in (€/KW) for a lifetime $T_{CHP-vie}$ in (hour)
C_{m-CHP} : Maintenance cost in (€/h)
C_{u-CHP}: Operating cost in (€/KWh)

- *For the power grid:*

$$C_{grid} = \sum_{t=1}^{24} C_{u-grid}.A_2(t).P_{grid}(t) \quad (32)$$

C_{u-grid} : Operating cost in (€/KWh)

- *For batteries:*

$$C_{batt} = \sum_{t=1}^{24} \frac{C_{I-batt}(P_{batt-crête},t)}{T_{batt-vie}}.t \quad (33)$$

C_{I-batt} : The total investment cost in (€/KW) for a lifetime $T_{batt-vie}$ in (hour)

The total cost is the sum of the costs for each production subsystem:

$$C_{total} = \sum_{t=1}^{24} \frac{C_{I-PV}(P_{PV-crête},t)}{T_{PV-vie}}.t + \sum_{t=1}^{24} C_{m-PV}.A_1(t).P_{PV}(t) + \sum_{t=1}^{24} \frac{C_{I-CHP}(P_{CHP-crête},t)}{T_{CHP-vie}}.t + \sum_{t=1}^{24} C_{m-CHP}.A_3(t).P_{CHP}(t) + \sum_{t=1}^{24} C_{u-CHP}.A_3(t).P_{CHP}(t) + \sum_{t=1}^{24} C_{u-GRID}.A_2(t).P_{grid}(t) + \sum_{t=1}^{24} \frac{C_{I-batt}(P_{batt-crête},t)}{T_{batt-vie}}.t \quad (34)$$

5. Problem statement and constraints

5.1. Energy optimization in a hybrid production system

The overall optimization of the energy supplied by the hybrid system's production sources is based on mathematical modeling of all the devices making up the system's energy chain (CHP, photovoltaic, battery, power grid). This is defined by mathematical equations reflecting the operation of the energy chain called "constraints" and control or decision variables and a cost function to be optimized called the "objective function". The type of modeling adopted depends once on the nature of the sources, and their characteristics such as: efficiency, energy losses… [34][35]. however, the resulting mathematical model can be expressed in different forms: linear, non-linear, convex or non-convex. Depending on the type of modeling, several methods or approaches exist to obtain optimal or sub-optimal decisions within calculation times that depend on the complexity of the mathematical model

[35]. The objective of this section is to minimize the cost of operating the system according to a given type of mission profile.

- *Photovoltaic system:* In our model, the renewable energy $P_{ER}(t)$ is first used as a source of electricity for the users because it is free of charge. Let $P_{PV}(t)$ be the renewable energy used to meet the electricity demand. If we have a surplus of renewable energy when the energy demand has been met, we use this part of the energy $P_{PV'}(t)$, to charge the batteries. In addition, the amount of renewable energy harvested in a time slot is limited.

$$P_{ER}(t) = P_{PV}(t) + P_{PV'}(t) \quad (34)$$

$$0 \leq \mathrm{P_{ER}(t)} \leq \mathrm{P_{ER\text{-}max}} \quad (35)$$

$$P_{PV}(t) = A_1(t).\,\eta_1.\big(1 - u_1(t)\big).P_{ER}(t) \quad (36)$$

$$P_{PV'}(t) = A_1(t).\,\eta_1.u_1(t).P_{ER}(t) \quad (37)$$

- *Local cogeneration unit:* We assume that electricity and thermal energy can be produced simultaneously by our local generator. Using an idealized model, we will investigate a more practical cogeneration model in our future work. η_e and η_h are the efficiencies of converting fuel to electricity and thermal energy respectively. At each time slot t, the cogeneration unit produces electricity and thermal energy, the quantities of which are designated respectively by $\eta_{e-CHP}.P_{CHP}(t)$ and $\eta_{h-CHP}.P_{CHP}(t)$. The electricity produced by the CHP denoted $P_{CHP}(t)$ will be used for power supply to meet the demand, with parameter $A_3(t)$ representing the on/off decision of the generator :
  - $A_3(t) = 1$: Represents the on/off of the cogeneration unit to the micro-grid
  - $A_3(t) = 0$: Refers to the micro-grid shutdown of the cogeneration unit.

$$P_{CHP'}(t) = \eta_{e-CHP}.P_{CHP}(t) \quad (38)$$

$$0 \leq P_{CHP}(t) \leq P_{CHP-max}(t) \quad (39)$$

$$P_{e-CHP}(t) = A_3(t).\,\eta_2.P_{CHP'}(t) \quad (40)$$

- *Centralized power grid:* We assume that the power grid and the micro-grid are connected. Electricity can be acquired from the centralized power grid to meet the demand for electricity. The system obtains power of the order of $P_{grid}(t)$ to meet the demand directly, where $P_{grid-max}$ is defined as the upper limit of direct power supply from the power grid. We then have:

$$0 \leq P_{grid}(t) \leq P_{grid-max} \quad (41)$$

$$P_{grid'}(t) = A_2(t).P_{grid}(t) \quad (42)$$

$$0 \leq P_{grid'}(t) \leq P_{grid'-max} \quad (43)$$

5.2. Balance of energy flows

The hybrid system to be designed consists of photovoltaic panels characterized by a total peak power P_{peak}, and an N_{CHP} number of CHP generators of the same size $P_{eCHP}(t)$. Since the system is designed to supply an entire electrical load $P_c(t)$, the following energy flow balance is available at any time t:

$$\sum P(t) = 0 \qquad P_{PV'}(t) + P_{c'}(t) - P_c(t) = 0 \tag{44}$$

$P_{PV'}(t)$: Total electrical power provided by the photovoltaic panels (KW)
$P_{c'}(t)$: Total electrical power supplied by CHP generators, batteries and power grid (KW)

5.3. Electricity demand

In our micro-grid system, $P_c(t)$ represents the total demand for electricity at time interval t, which must be met once requested. The net power demand $P_{c'}(t)$, which is the excess of the power demand over the renewable energy at time interval *t*, is equal to the subtraction of the power demand and the renewable energy, and can be expressed as:

$$P_{c'}(t) = P_c(t) - P_{PV'}(t) \tag{45}$$

The Pc-max indicates the maximum net power demand in a time interval, and then we have:

$$0 \le P_{c'}(t) \le P_{c-max} \tag{46}$$

The power can be obtained from the electrical grid, the local cogeneration plant and the battery, designated by: $P_{grid'}(t), P_{CHP'}(t),\ P_{b'}(t)$.

$$P_{c'}(t) = P_{grid'}(t) + P_{CHP'}(t) + P_{b'}(t) \tag{47}$$

$$P_{c'}(t) = A_2(t).P_{grid}(t) + A_3(t).\eta_2.P_{CHP}(t) + A_4(t).\eta_3.P_b(t) \tag{48}$$

5.4. Battery charging and discharging model

The dynamics of the battery state of charge (SOC) level $B(t)$ is given as follows :

$$B(t) = B(t-1) - \eta_D.P_{b'}(t) + \eta_c.P_{PV'}(t) \tag{49}$$

$$B(t) = B(t-1) - \eta_D.\left[A_4(t).\eta_3.P_b(t)\right] + \eta_c.[P_{PV'}(t)] \tag{50}$$

Where η_D is the discharge efficiency of the battery; and η_c is the charge efficiency of the battery. We can see that the battery must satisfy capacity and charge/discharge constraints at any time t.

$$0 \le P_B(t) \le P_{44max} \tag{51}$$

$$0 \le P_{B'}(t) \le P_{charge} \tag{52}$$

The energy accumulator here is of the electrochemical type characterized by its maximum storage capacity B_{max}, efficiency η_4, availability $A_4(t)$. We note $B(t)$ the energy stored in the battery and $P_b(t)$ the power it receives or supplies at time *t*.

$$P_{b'}(t) = A_4(t).\eta_3.P_b(t) \tag{53}$$

$$B_{min} \le B(t) \le B_{max} \tag{54}$$

Where B_{max} is the battery capacity, P_{44max} is the maximum discharge power of the battery in each time slot, and P_{charge} is the maximum charge power of the battery.

5.5. Consumption profiles: On-site consumption data

In our case study we will provide consumption data of a collective room with a one hour step during a basic test day. Note that the premise under consideration has a surface area of 200 m² for about ten inhabitants. With such consumption profiles it is interesting to have an overview of the measurements. Daily curves are presented in winter and summer with a fall in consumption during the weekend compared to the days worked during the week when consumption is interesting during opening hours. One will notice basic power consumption even during the night around 2.2KW for the summer season and 4KW for the winter season, which should correspond to the air conditioning or heating system and the monitoring systems of the refrigerating appliances.

5.6. Production profiles: Photovoltaic panel model

To generate a production profile of a photovoltaic system, we use a simple model of solar panels inherited from a one-diode representation. The calculation of the power produced takes into account the incident sunlight, and the ambient temperature according to the characteristics of the panels considered.

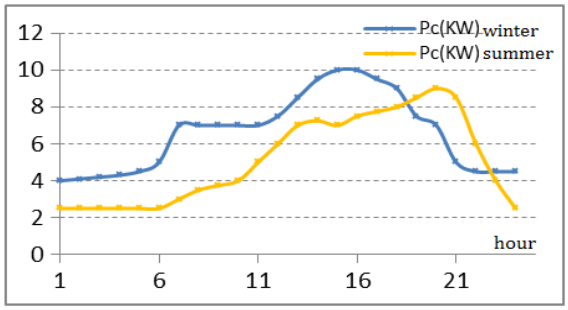

Figure 13: consumption data in KW: winter/summer season

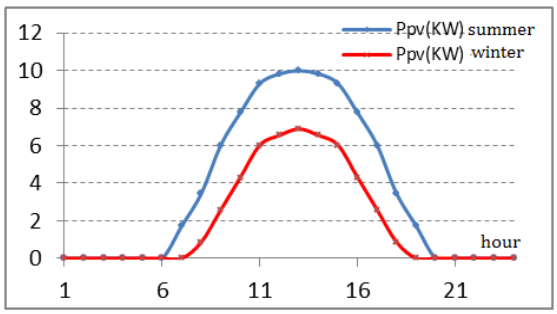

Figure 14: power produced by the photovoltaic system winter/summer

5.7. The objective functions of the problem

The objective function of the constrained minimization problem is the total discounted cost just taking into account the costs of using each production system at the end of the time horizon [35]. For reasons of complexity, a discretization of space-time is performed with a time step $\Delta t=1h$. All these vectors are sampled per hour (24 points for a full day). By associating the objective and the constraints related to the operation of the system, the global model is as follows:

$$f(t) = C_{U-PV}P_{PV}(t) + C_{U-grid}P_{grid}(t) + C_{U-CHP}P_{CHP}(t) + C_{U-batt}P_{batt}(t) \quad (55)$$

$$\text{Objectif: } min \sum_1^{24} f(t) \quad (56)$$

$$P_c(t) = P_{PV'}(t) + P_{grid'}(t) + P_{CHP'}(t) + P_{B'}(t) \qquad \forall t \in T \quad (57)$$

$$P_{c'}(t) = P_c(t) - P_{PV'}(t) \qquad \forall t \in T \quad (58)$$

$$B(t) = B(t-1) - \eta_D . P_{B'}(t) + \eta_c . P_B(t) \qquad \forall t \in T \qquad (59)$$

$$0 \leq B(t) \leq B_{max} \qquad \forall t \in T \qquad (60)$$

$$0 \leq P_{c'}(t) \leq P_{c'-max} \qquad \forall t \in T \qquad (61)$$

$$0 \leq P_{PV}(t) \leq P_{PV-max} \qquad \forall t \in T \qquad (62)$$

$$0 \leq P_{grid}(t) \leq P_{grid-max} \qquad \forall t \in T \qquad (63)$$

$$0 \leq P_{CHP}(t) \leq P_{CHP-max} \qquad \forall t \in T \qquad (64)$$

$$0 \leq P_{B'}(t) \leq P_{B'-max} \qquad \forall t \in T \qquad (65)$$

$$P_{B-min} \leq P_B(t) \leq P_{B-max} \qquad \forall t \in T \qquad (66)$$

The state vectors are: $S_t = \left[P_c(t), P_{PV}(t), B(t), C_{grid}(t), C_{CHP}(t)\right]$
The control vectors are : $U_t = \left[P_{PV'}(t), P_{grid'}(t), P_{CHP'}(t), P_{B'}(t)\right]$

The optimization parameters are, for each hour, the energy produced by the photovoltaic system, the cost of purchasing electricity from the grid, the cost of purchasing fuel for the cogeneration unit, and the electrical demand (load profile). The optimization variables are the peak power of the photovoltaic field, the maximum power supplied by the electrical grid, and the installed power of the CHP generators. These three variables are sufficient to fully determine the system characteristics.

5.8. Strategies and control algorithm for energy management

In order to perform an energy balance calculation at all levels of the system, the user must provide estimates of final energy demands [36][37]. It must also provide the capacities of the existing installations, the characteristics and potentials of the technologies used. These data are then converted into matrices, corresponding to a linear-mixed programming problem whose objective function is the constrained minimization of the total discounted cost. Optimization algorithms are at the center of the management strategies envisaged and aim in a large part of the studies to enhance the value of the multi-source system by minimizing the energy bill. A number of methods can be found in the literature for optimal management of energy flows. Two main classes emerge between step-by-step optimization procedures of references for degrees of freedom or a global optimization of flows over a given planning window.

Towards a linear modeling in mixed variables:
Linear programming deals with a particular class of convex optimization problems, where the objective function and all constraint functions are linear [38]. The solution of linear optimization problems is obtained more easily than that of non-linear problems.

$$\min \overrightarrow{f}.\overrightarrow{x}, \overrightarrow{f}, \overrightarrow{x} \in \mathbb{R}^n$$

$$A_{eq}.\overrightarrow{x} = \overrightarrow{b_{eq}} \quad , \quad A_{eq} \in \mathbb{R}^{p \times n} \quad , \quad \overrightarrow{b_{eq}} \in \mathbb{R}^p$$

$$A_{neq}.\overrightarrow{x} \leq \overrightarrow{b_{neq}} \quad , \quad A_{neq} \in \mathbb{R}^{q \times n} \quad , \quad \overrightarrow{b_{eq}} \in \mathbb{R}^q$$

Algorithms exist which find a solution to the linear problem under constraints in polynomial time or prove that such a solution does not exist. Two classes of methods group the most popular algorithms. Both can be characterized as linear search methods [38]:
- The algorithms based on the Danzig simplex algorithm are based on the idea that linear constraints define a convex polytope in $\mathbb{R}$. If a solution exists, it is located at a vertex of this polytope. The simplex algorithm progresses by evaluating a subset of the vertices. It moves from one vertex of the convex envelope to a neighboring vertex, always reducing the objective value.
- On the contrary, the inner point algorithms construct a sequence of points within the allowable space following a descending direction of the objective function while keeping an appropriate distance from its bounds at each iteration.

6. Case study: Study and optimization of the system without storage unit

In this case the storage system is cancelled, the three distributable sources, the photovoltaic system, the cogeneration unit, and the power grid, represented by $P_{PV}(t)$, $P_{CHP}(t)$ and $P_{GRID}(t)$, are used to supply the load, when the load demand exceeds the limit of the photovoltaic system. The problem is to minimize the cost of operating these generation units for a specific operating period in order to meet the system load demand and the operational constraints of the power system to be maintained.

$$\text{Objectif: } min \sum_1^{24} f(t) \tag{67}$$

$$f(t) = C_{U-PV}P_{PV}(t) + C_{U-grid}P_{grid}(t) + C_{U-CHP}P_{CHP}(t) \tag{68}$$

$$P_c(t) = P_{PV'}(t) + P_{grid'}(t) + P_{CHP'}(t)\ ; \tag{69}$$

(58), (61), (62), (63), (64)

$$A_1(t) = A_2(t) = A_3(t) = 1 \quad , \quad A_4(t) = 0 \tag{75}$$

The state vectors are: $S_t = \left[P_c(t), P_{PV}(t), C_{grid}(t), C_{CHP}(t)\right]$

The control vectors are: $U_t = \left[P_{PV'}(t), P_{grid'}(t), P_{CHP'}(t)\right]$

The entire management procedure is summarized in the diagram in Figure 4. Starting from the optimal demand specifications and production/cost measures, optimizations are initiated according to the target value in relation to the optimal profile. Once these procedures have been carried out, the new grid and cogeneration unit capacities are calculated based on the adopted management program.

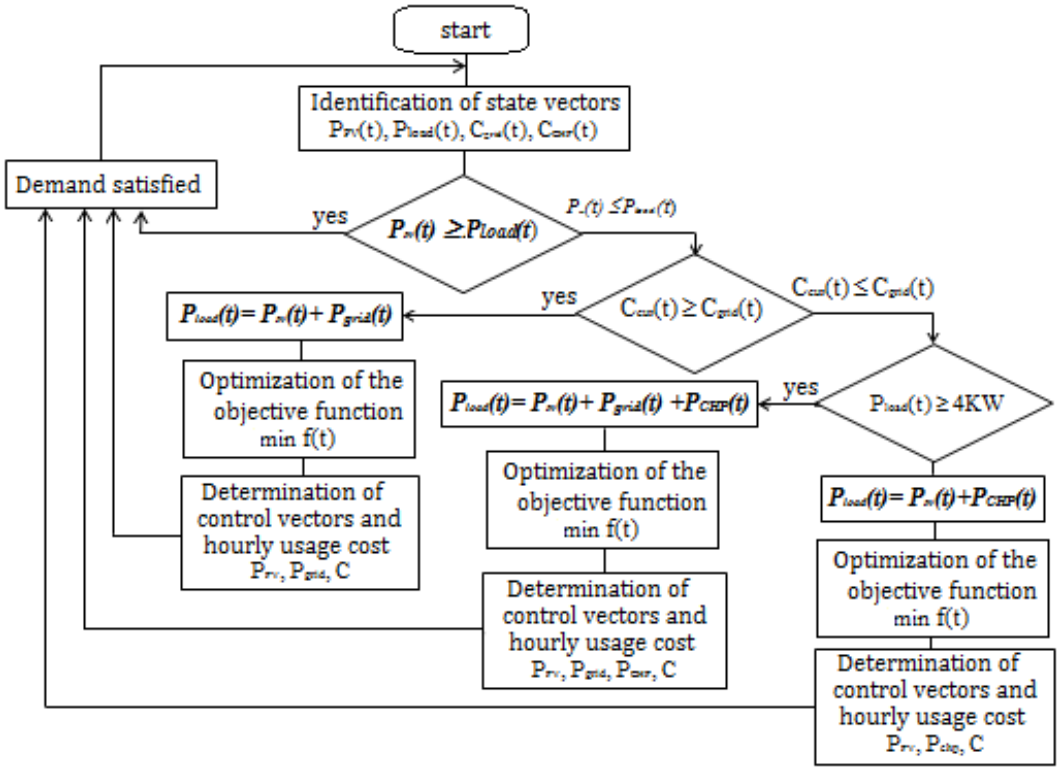

Figure 15: flowchart of the non-storage mode in which all the conditions for optimization are ensured

Simulation Results:

The simulation of the process is carried out on the basic test day (winter/summer working day) used as a basis for the management system, taking into account the production/cost constraints. The corresponding consumption and production profiles are given in Figures 2 and 3. Daily operation of the optimal system: Figure 3.4 shows the daily production of the PV field, the cogeneration unit, and the power grid on a typical day. It can be seen that the demand is satisfied at each instant t by the sum of the powers at the same instant t that pose a minimum cost of use (which confirms the energy balance).

It is therefore important to point out that the energy produced by PV has smoothed the consumption curve well during sunny periods, especially in summer (low consumption) with fewer hours of operation of the cogeneration unit. On the other hand, during the winter months, it can be seen that another source with PV is needed to satisfy the electrical demand.

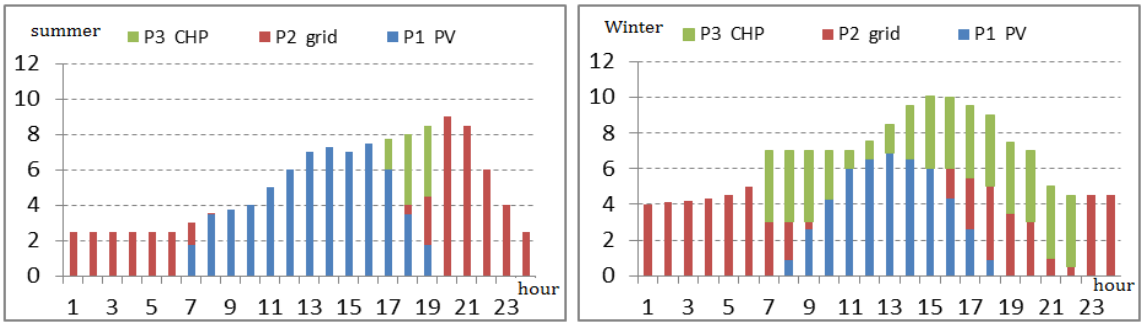

Figure 16: Simulation results for summer/winter source balancing

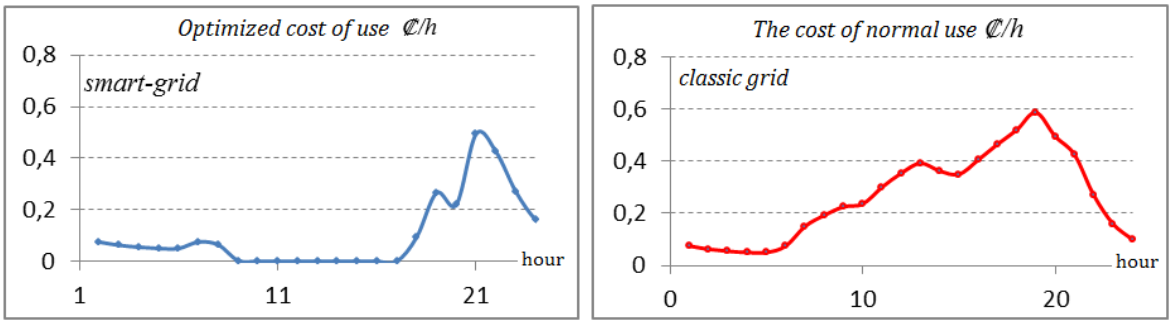

Figure 17: Summer hourly usage cost - smart-grid/classical

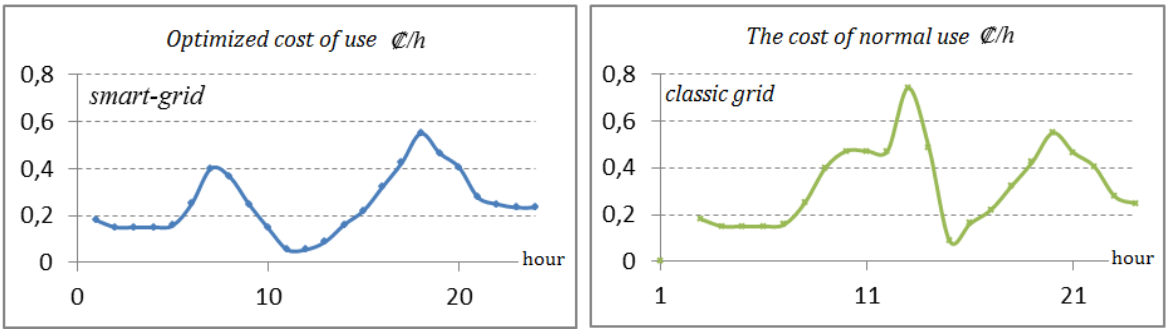

Figure 18: Winter hourly usage cost - smart-grid/classical

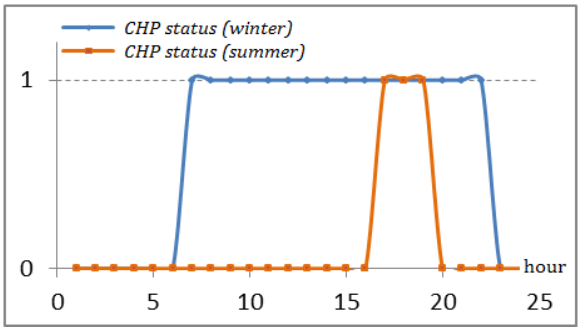

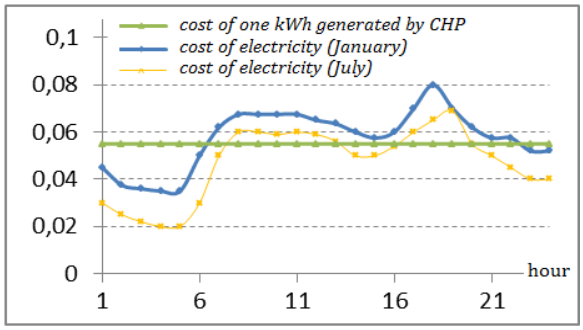

Figure 19: Status of the cogeneration unit (1=ON, 0=OFF) Figure 20: winter/summer electricity costs

Interpretations:

The use of a cogeneration unit (CHP) as a complementary agent in a hybrid system comprising a photovoltaic production line and a conventional source (figure 16) represents an interesting solution to the problem of peak hours when the demand for energy is high (figure 19), especially during the coldest hours, CHP allows to replace during hours of the day the direct consumption through the electrical grid with a lower cost. In order to illustrate (figure 17, 18) the gains brought by the integration of a CHP unit and a solar field in an electric grid, this integration brings a saving in the tariffs imposed by the public producer (conventional consumption). The influence of the integration on the hourly use cost curve can be seen in the periods between 5 a.m. and 9 p.m. during the summer, and during periods of high consumption (in winter) between 12 noon and 8 p.m. The energy management applied to the system has made it possible to reduce the energy supplied by the electrical network, with a saving of 22.9% in bills during the winter period and 61.2% during the summer period, showing the particular interest of the management strategy when the system is subsidized by other production systems.

Conclusion

In this work, a general presentation of energy production systems was the subject of a first part. The characteristics of the elements making up the power system were briefly presented, including their modeling and numerical simulation. Then, an economic model of the production system was presented to evaluate the cost of operating the system in comparison with a conventional production system. Before developing the optimization algorithms required for management and sizing, the energy flows of each subsystem studied must be defined in a manner appropriate to the level of precision compatible with the optimization procedures to be implemented subsequently. The second part is devoted to the definition of the input data (climatic potential, consumption profile, etc.) as well as the envisaged tariff policies. These data will be essential to test the algorithms set up, and to propose energy management and optimization methods adapted to multi-source systems able to meet the energy demand at each time interval while respecting the various constraints related to the operation of the system's energy chain, and to minimize and optimize fuel consumption by conventional sources (cogeneration unit). The simulation results obtained showed the primary interest of integrating renewable generation sources in a hybrid system, by minimizing the dependence on the electrical grid and the fluctuation of consumption rates. The connection of a cogeneration unit to the hybrid system plays an interesting role during peak hours when electricity costs are important.

Acknowledgements

The research team would like to thank the national center for scientific and technical research CNRST, for its funding of the project "Study of appropriate technologies for the conversion of organic waste and biomass into renewable energy and sustainable bio-fertilization

Notation

E_s : Sunlight in the plane of the panels (W/m^2)
T_j : Cell junction temperature (°C)
I_G : Current GI supplied by the panel group (A)
V_G : Voltage at the group terminals (V)
E_{ref} : Corresponds to the reference sunshine of 1000W/m^2
T_{jref} : The temperature of the reference panels of 25°C.
P_1, P_2, P_3, P_4 : are constant parameters.
k : Boltzmann constant (1.38.10^{-23} J/K),
q : The elementary load (1.6 10^{-19} C), and
E_g : Gap energy
Ns : nombre des panneaux montés en série
A : surface d'un panneau
Rsh : résistance de shunt
Rs : résistance equivalent
P_{MPPT} : Power supplied by the PV field (W)
N_{PV} : Number of modules in the PV field

G_I : Global solar irradiation of the considered place (W.m-2)
G_I^R : Global solar irradiation under reference conditions (=1000W.m-2)
P_{max} : Peak power of a PV module under reference conditions (Wp)
μ_{max} : Variation of PV power as a function of temperature
T_J : PV module junction temperature
T_J^R : Junction temperature in the reference conditions of the module (=25C°)
T_A : Ambient temperature of the place under consideration (C°)
$NOCT$: Operating temperature of PV cells under reference conditions (C°)
C_{batt} : Total battery capacity (Ah)
$E_c(t)$: Daily consumption
V_{batt} : Output voltage of the battery bank (V)
η_{batt} : Battery efficiency.
DOD : Represents the permissible deep discharge of the battery (Depth of Discharge).
J : Number of days of autonomy
C : The dynamics of the mechanical torque
K : The static gain
T_r : Time constant expressing the limit in reaction speed of the motor
T_c : Time constant expresses the time delay for the
$m_B(s)$: The equivalent in the Laplace plane of the supply index.
ω_{mref} : The rotational speed
S_{ref} : The basic apparent power
H_D : total inertia
D_D : total friction coefficient
V_S^{abc} : Stator voltages
V_r^{abc} : Rotor voltages
R_s : Stator resistor
R_r : Rotor resistor
Is : Stator currents
Ir : Rotor currents
C_{em} : Electromagnetic torque
P_g : Instantaneous electrical power
φ_s^{abc} : Stator flux
φ_r^{abc} : Rotor flux

References

[1] M. Muselli, G. Notton, and A. Louche, “design of hybrid-photovoltaic power generator, with optimization of energy management,” Sol. Energy, vol. 65, 1999.
[2] M. REMY RIGO-MARIANI, thèse de doctorat « méthodes de conception intégrée "dimensionnement gestion" par optimisation d'un micro-réseau avec stockage », Université de Toulouse, 2014
[3] P. Bajpai and V. Dash, “Hybrid renewable energy systems for power generation in stand-alone applications: A review,” Renew. Sustain. Energy Rev., vol. 16, no.5, pp. 2926–2939, juin 2012.
[4] Y. S. Mohammed, M. W. Mustafa, and N. Bashir, “Hybrid renewable energy systems for off-grid electric power: Review of substantial issues,” Renew. Sustain. Energy Rev., vol. 35, juillet 2014.
[5] Guanglin Zhang article Optimal Energy Management for Microgrids with Combined Heat and Power (CHP) Generation, Energy Storages, and Renewable Energy Sources, Energies 2017 journal of MDPI.
[6] Arnaud VERGNOL "Intégration dans le réseau électrique et le marché de l’électricité de production décentralisée d’origine renouvelable : Gestion des congestions locales". Thèse préparée dans le Laboratoire d’Electrotechnique et d’Electronique de Puissance de Lille. 2010
[7] MOHAMED MLADJAO Mouhammad Al anfaf rapport de thèse “contribution à la modélisation et a l’optimisation de systèmes énergétiques multi-sources et multi-charges », Ecole Doctorale «Sciences et Ingénierie Ressources Procédés Produit Environnement ». 2016

[8] CHRISTOPHE DARRAS, rapport de thèse « Modélisation de systèmes hybrides Photovoltaïque / Hydrogène : Applications site isolé, micro-réseau, et connexion au réseau électrique dans le cadre du projet pepite», universite de corse-pascal paoli, école doctorale environnement et société, faculté ST. 2010

[9] Nfah, E.M., Ngundam, J.M., Tchinda, R. Modelling of solar/diesel/battery hybrid power systems for far-north Cameroon. Renewable Energy, vol. 32, pp. 832-844, 2007.

[10] Olivier GERGAUD, rapport de thèse « Modélisation énergétique et optimisation économique d'un système de production éolien et photovoltaïque couplé au réseau et associé à un accumulateur», thèse de doctorat de l'école normale supérieure de cachan, 2002

[11] Bhave, A. G., (1999). Hybrid solar-wind domestic power generating system-a case study. Renewable Energy, vol. 17, pp. 355-358, 1999.

[12] David Blaise TSUANYO, thèse de doctorat « Approches technico-économiques d'optimisation des systèmes énergétiques décentralisés: cas des systèmes hybrides PV/Diesel », université de perpignan via domitia, 2015

[13] Perlman, J., McNamara, A., Strobino, D., (2005). Analysis of PV system performance versus modeled expectations across a set of identical PV systems. ISES 2005 Solar World Congress, 2005.

[14] Muselli, M., Notton, G., Poggi, P., Louche, A.. PV-hybrid power systems sizing incorporating battery storage: analysis via simulation calculations. Renewable Energy, vol. 20, pp. 1-7, 2000.

[15] Hamidat, A., Benyoucef, B., (2008). Mathematic models of photovoltaic motor-pump systems. Renewable Energy, vol. 33, pp. 933–942, 2008.

[16] S. Chen, P. Li, D. Brady, and B. Lehman, "Determining the optimum grid connected photovoltaic inverter size," Sol. Energy, vol. 87. 2013.

[17] M. A. M. Ramli, A. Hiendro, K. Sedraoui, and S. Twaha, "Optimal sizing of gridconnected photovoltaic energy system in Saudi Arabia," Renew. Energy, vol. 75, pp. 489–495, Mar. 2015

[18] Douangsyla, S., Indarack, P., Kanthee, A., Kando, M., Kittiratsatcha, S., Kinnares, V., (2004). Modeling for PWM Voltage Source Converter Controlled Power Transfer. Proceedings of International Symposium on Communications and Information Technologies, pp. 875-878, 2004

[19] Rosell, J.I., Ibarñez, M., (2006). Modelling power output in photovoltaic modules for outdoor operating conditions. Energy Conversion and Management, vol. 47, pp. 2424–2430, 2006.

[20] M. G. Kratzenberg, E. M. Deschamps, L. Nascimento, R Rather, and H. H. Zern, "Optimal Photovoltaic Inverter Sizing Considering Different Climate Conditions and Energy Prices," Energy Procedia, vol. 57. 2014

[21] Schmid, J., Von Dincklage, R.D., (1988). Power Conditioning and Control. Euroforum New Energies, Saarbruken, Germany, 241-243, 1988.

[22] Schmid, J., Schmidt, H., (1991). Inverters for Photovoltaic Systems. 5th Contractor's Meeting of the EC Photovoltaic Demonstration Projects, Ispra, Italy, pp. 122-132, 1991.

[23] C. V. Nayar, "Recent developments in decentralised mini-grid diesel power systems in Australia," Appl. Energy, vol. 52, no. 2–3, 1995.

[24] K. Wadumesthrige, N. Johnson, M. Winston-Galant, S. Zeng, E. Sattler, S. O. Salley, and K. Y. Simon Ng, "Performance and durability of a generator set CI engine using synthetic and petroleum based fuels for military applications," Appl. Energy, vol. 87, no. 5, pp. 1581–1590, 2010.

[25] IEEE Std 421.5TM,"Recommended Practice for Excitation System Models for Power System Stability Studies", IEEE Power Engineering Society, 2005

[26] D. Yamegueu, Y. Azoumah, X. Py, and N. Zongo, "Experimental study of electricity generation by Solar PV/diesel hybrid systems without battery storage for off-grid areas," Renew. Energy, vol. 36, 2011.

[27] Rachid Maamri "Modélisation et expérimentation des moteurs à combustion fonctionnant avec différents carburants de substitution et mélanges". Université du Québec 2014

[28] Willard W. Pulkrabek, "Engineering Fondamentals of the Internal Conbustion Engine", Prentice Hall. 2003

[29] Prabha Kundur, "Power Systems Stability and Control", Electric Power Reserch Institute".1994

[30] D. B. Hulwan and S. V. Joshi, "Performance, emission and combustion characteristic of a multicylinder DI diesel engine running on diesel–ethanol–biodiesel blends of high ethanol content," Appl. Energy, vol. 88, no. 12, pp. 5042–5055, Dec. 2011.

[31] T. Daho, G. Vaitilingom, S. K. Ouiminga, B. Piriou, A. S. Zongo, S. Ouoba, and J. Koulidiati, "Influence of engine load and fuel droplet size on performance of a CI engine". 2013

[32] Shaahid, S.M., Elhadidy, M.A., (2003). Opportunities for utilization of stand-alone hybrid (photovoltaic, diesel, battery) power systems in hot climates. Renewable Energy, vol. 28, pp. 1741–1753, 2003.

[33] Ludmil Stoyanov, thèse de doctorat « Etude de différentes structures de systèmes hybrides à sources d'énergie renouvelables », université technique de SOFIA, 2011

[34] J. L. Bernal-Agustín and R. Dufo-López, "Simulation and optimization of stand-alone hybrid renewable energy systems," Renew. Sustain. Energy Rev., vol. 13, no. 8, pp. 2111–2118, Oct. 2009.

[35] R. Dufo-Lopez and J. L. Bernal-Agustín, "Design and control strategies of PV-Diesel systems using genetic algorithms," Sol. Energy, vol. 79, no. 1, pp. 33–46, 2005.

[36] R. Baños, F. Manzano-Agugliaro, F. G. Montoya, C. Gil, A. Alcayde, and J. Gómez, "Optimization methods applied to renewable and sustainable energy: A review," Renew. Sustain. Energy Rev., vol. 15, no. 4, pp. 1753–1766, mai 2011.

[37] Pierre-Louis Poirion, thèse de doctorat « Programmation linéaire mixte robuste; Application au dimensionnement d'un systéme hybride de production d'électricité », École doctorale informatique, télécommunication et électronique (paris), 2013

[38] R. Dufo-López, J. L. Bernal-Agustín, J. M. Yusta-Loyo, J. A. Domínguez-Navarro, I. J. Ramírez-Rosado, J. Lujano, and I. Aso, "Multi-objective optimization minimizing cost and life cycle emissions of stand-alone PV–wind–diesel systems with batteries storage," Appl. Energy, vol. 88, no. 11, Nov. 2011.